SRI DHARMASTHALA MANJUNATHESHWARA COLLEGE
(Autonomous) UJIRE – 574 240
(Re-Accredited 'A' Grade with CGPA 3.59 by NAAC)

Minor Research Project
On

SYNTHESIS AND CHARACTERIZATION OF NON LINEAR OPTICAL MATERIALS

Submitted to

University Grants Commission
South Western Regional Office
Bangalore

By

Prof. B. Ganapayya
Principal Investigator

And

Prof. Shiva Rao
Co-investigator

Department of Physics
SDM College (Autonomous)
Ujire – 574 240

June 2013

Certificate

We hereby declare that the minor research project entitled "SYNTHESIS AND CHARACTERIZATION OF NON LINEAR OPTICAL MATERIALS" has been carried out by us in the Department of Physics of our college granted by University Grants Commission, New Delhi

We further declare that the work contained in this report has not formed the basis for the award any degree of any university.

Ujire
30-6-2013

Prof. B. Ganapayya

Prof. Shiva Rao

Acknowledgement

We are grateful to the management of SDME Society, particularly president of the Institution **Dr. D. Veerendra Heggade**, Vice president secretaries and **Dr. B.Yashovarma**, Principal of the institution for all the encouragement and timely support.

The **University Grants Commission** provided us the crucial support that made this project a reality. We acknowledge our indebtedness to the joint Secretary and Regional Head of UGC, Bangalore.

We feel great pleasure in expressing our sincere thanks to all those who helped directly and indirectly in completing this work.

We are equally grateful to teaching and non teaching staff of our department for their timely help to complete our work.

We are happy to place on record the help and support extended by our family members and friends to complete the project.

Prof. B. Ganapayya

30-6-2013 **Prof. Shiva Rao**

CONTENTS

CHAPTER – 1

INTRODUCTION

Nonlinear optics is expected to play a major role in the technology of photonics, which is emerging as multidisciplinary new frontier of science and technology that is capturing the imagination of scientists and engineers worldwide because of its potential applications to many areas of present and future information and image processing technologies. Examples for nonlinear optical phenomenon that are potentially useful in this context are the ability to alter the frequency or color of light and so amplify one source of light with another. Switch it, or alter its transmission characteristics through a medium depending on its intensity. It is the potential for providing these functions in suitable materials and devices that motivates much of the current fundamental and exploratory research in the field of nonlinear optics.

There is considerable interest in the synthesis of new materials with large order optical nonlinearities, because of their potential for use in applications including telecommunications optical computing, optical data storage and information processing. Organic crystals are increasingly being recognized as “materials of future” because of their molecular nature combined with versatility of synthesis, can be used to alter and optimize their molecular structure in order to optimize their nonlinear optical (NLO) properties. These nonlinear optical properties can exceed those of inorganic crystals. The organic NLO crystals are promising candidates for frequency-

doubling applications in lasers. The suitability of a crystal in a nonlinear optical device depends on its properties. High molecular hyperpolarizability and acentircity of the crystal structure are mandatory for a material to be used in nonlinear optical devices. The quality of a crystal depends on the conditions of its growth. The difficulty in growing large size, good quality organic single crystals with required processiblity and environmental stability, has not yet overcome completely. Hence there is a need for the study of crystal growth of new nonlinear optical organic materials and the characterization of these single crystals. The organic nonlinear optical materials have good nonlinear optical susceptibilities but low laser damage threshold value in comparison with inorganic counterparts. So, in order to satisfy the day to day technological requirements, new nonlinear optical materials are mandatory.

Nonlinear optics (NLO) has wide applications in the field of telecommunication and optical information storage devices. The organic NLO materials play an important role in SHG, frequency mixing; electro optic modulation, optical parametric oscillation, optical bistability etc.

CHAPTER – 2

DIFFERENT METHODS OF CRYSTAL GROWTH

Crystals have interested man because of their beauty and rarity since prehistoric times, but their large scale use has been brought about mainly by the demands of solid state materials for research and devices. Now a days the study of growth and characterisation of single crystals is receiving increasing importance due to their large number of applications in Electronics, Lasers, non-linear optics, Electro-mechanical trans devices, Radiation detectors, Electro-luminescent devices etc. Many properties of solids are best studied with single crystals. As a result a large amount of labour and care have been lavished on the development of different growth techniques, each having its own importance and potentialities.

Different methods of growing crystals have been reviewed by Brice , Pamplin, Patel and others.

Mainly there are three categories of crystal growth processes.

(1) A change from one solid phase to another is accompanied by change in the crystal structure - solid growth.

(2) A change from the liquid phase to the solid -crystallization occurs from a melt or solution growth.

(3) A change from gaseous phase to the solid recrystallization occurs by sublimation- vapour growth.

2.1 Solid Growth:

Growth from solid phase has different methods like, recrystalization by annealing out strain, sintering, polymorphic phase transition, solid state

precipitation etc. This process is rarely used except for certain metals where strian annelaing is effective and• in certain cases where crystal structure change occurs, between the melting point and room temperature. The main disadvantage is that the density of sites for nucleation is high and it is difficult to control nucleation to produce large single crystals.

2.2 Growth From Melt

It is essentially growth by controlled freezing and in comparison to other growth methods is an uncomplicated, readilly controllable process. All materials which melt congruently, do not decompose before melting and do not undergo a phase transition between melting point and room temperature, are grown as single crystals by this method.

The material to be grown in the form of single crystals is placed in a suitable container and heated in a furnace above the melting point. Growth will normally start when the temperature is slightly below the equilibrium melting point. , Usually crystals grow most rapidly in certain crystallographic direction. It is difficult to control the rapid transition from molten state to the solid.

Crystal growth from melt can be achieved by different techniques depending on the specific properties of the material and required size and shape. The methods of growing crystals from melt may be devided into four types.

(1) Bridgeman - Stockbargers technique.

(2) Czochralski - Crystal pulling (czochralski)

(3) Zone melting.

(4) Verneuil flame fusion technique.

The inorganic crystals like ruby [alkali halides] , semiconductor crystals GaAs[GaP etc. and organic crystals like urea NPAN , DAN , MNA etc. are grown by this method.

2.3 Growth from the Vapour Phase

Materials which decompose or sublime before melting at atmospheric pressure and when a suitable solvent is not available, crystals can be grown from the vapour phase. Most available crystals can be grown from the vapour phase. Most of the semi conducting crystals have been grown by this method. This method has been employed to produce bulk crystals to produce their films on crystals prepared by other techniques semi conductor devices and integrated circuits. Crystals grown from vapour phase can readily lead to high purity materials.

Vapour growth processes may be divided into three main categories.

(1) Sublimation . in which a solid is passed down a temperature gradient and crystals grow from the vapour phase at the cold end of the tube.

(2) Vapour transport in which solid material is passed down the tube by a carrier gas.

(3) Gas phase reactions in which crystals grow as a product precipitated from the vapour phase as the direct result of a chemical reaction between vapour species.

Using this method single-crystals of Cd, Zn, Au, etc. can be grown.

2.4 Crystal Growth by Gel Method

Gel growth which can be regarded as an intermediate case between growth in the solid and in solution. It is a popular method used to obtain

pure crystals. This method relies on reaction and precipitation of species diffusing in gels.

Gel is a highly viscous two component system, semi solid in nature, rich in liquid. The materials which are ordinarily called gels include silica gel, gelatin, agar polyacrylamide and various hydroxides in water. Growth is usually limited by diffusion.

Silica hydrogel has been used as the best and most varsatile growth medium to grow good quality single crystals. Silica hydrogel is prepared by mixing aqueous solution of sodium meta silicate of specific gravity 1.03 to 1.06 with mineral or organic acid. The gelling process itself takes an amount of time which can vary widely from minutes to many days depending on the nature of the material and its temperature.

Gel method is useful for the growth of crystals which decompose at temperature below their melting point and also for those not having suitable solvents for recrystallization.

Crystals with demensions of several mm can be grown in periods of 2 to 3 weeks. The apparatus used are simple. The particular advantage of the method is that the growing crystal is held in the gel in a strain free manner.

Various types of crystals-ionic, organic, metallic and biological crystals have been grown by this method.

2.5 Growth of Single Crystals from Solution

Of all the methods of crystal growth solution growth is the most widely practiced, Growth from the solution is the only alternative, if the substance decomposes below its melting point or under goes a phase change. The choice of the solvent is probably the most critical step in solution

growth. The water is the best available solvent for many mateirals, the aqueous solution growth is restricted only to the water soluble materials. Sometimes it is more useful to use mixture of solvents.

Crystallization from solution usually takes place in a temperature range 0-100^0 C. Crystals grow from solution if the solution is supersaturated. Supersaturated solutions are generally unstable. A transition from the non-equillibrium to the equillibrium state is accompanied by crystallization.

The growth rates in this method are much smaller than the growth rates from melt. It is very difficult to avoid spontaneous nucleation in a solution method.

The supersaturation, the necessary condition for the crystallization, can be produced by any of the following methods.

2.5a . Evaporation Method

This method involves ordinary evaporation i.e. by removing the solvents by evaporation at constant temperature. The container having solvent is covered with a plate and the rate of evaporation is controlled by varying number of holes in plate used to cover the solution. More elegent method is to pass inert gas over the top of the liquid. The rate of evaporation is controlled by the rate of flow of gas.

Growth from evaporation will yield homogenous crystals provided that growth occurs at a temperature, when the solute composition is same in the solid and liquid phases. Crystals are more uniform in composition than those obtained by slow cooling.

The main disadvantage is due to the tendency of the crystals to nucleate at the surface of the solution, which frequently produces poor

quality crystals and at high temperatures it is due to corrosive nature of most of the solvents.

In this method large inorganic crystals like ADP, KDP, strontium formate, sodium formate and organic crystals like urea, NPPA, PNP are grown.

2.5b Slow Cooling

Of all the methods slow cooling is the easiest method for the growth of crystals from solution. In this method supersaturation is attained by using temperature dependence of solubility. If the solubility of the solute is increased with the rising temperature, we can prepare a saturated solution at high temperature and then slowly cool it. Since solubility decreases during this cooling, such solution becomes supersaturated. Very good quality crystals can be produced by the slowest cooling rates. Its principal disadvantage is the one which needs to use a range of temperature and any growth temperature dependent property will not remain uniform. The method also has technical difficulty of requiring a programmed temperature. The slow cooling can also be done at high temperatures but unseeded growth from flux at high temperature needs large supersaturation to produce initial necleation. This gives rapid growth initially with possibilities of many flux inclusions. Crystals like nickel oxide, megnesium ferrite and vanadate are grown by this method.

CHAPTER – 3

STRUCTURE AND PROPERTIES OF ORGANIC CRYSTALS

In most of the text books on solid state, molecular solids are given at most a few paragraphs, and organic crystals are never mentioned at all. This is unfortunate, since organic crystals have an enormous range of interesting properties that are almost continuously "tunable". For the last twenty five years there has been increasing awareness of these systems as their most interesting properties have been uncovered. For example, superconductivity, spinless conductivity in doped conj ugated polymers and large nonlinear optical responses.

Most organic solids are molecular solids; i.e., the molecules retain their geometric shape and properties to a large degree upon condensation from the vapour. Thus, benzeene, for example, is hexagonal in the crystal with only small changes from the gas-phase molecule. In addition, the infrared and low energy optical spectra of the solid are very similar to those of-the gas. Strictly speaking there may be few changes. However these changes are small compared to those occurring in typical ionic crystals or metals. Finally organic crystals have small cohesive energies. Therefore most organic crystals are collection of molecules held together by weak intermolecular interactions, usually described by Vander-Waals forces. The organic crystals often have more complicated structures, exhibit

polymorphism and many phase transitions, often have many structural defects.

Structural defects in molecular crystals are common point defects, such as misorientations, interstitials, vacancies and impurities are welknown. Extended defects such as dislocations are often found as well as stacking faults and others. Similarly polymorphic inclusions, and impurity aggregations are known. At present, very little is known about these defects except for their existence. These defects will cause the electronic states of the ideal crystal to be perturbed and perhaps be localised; they will cause inhomogeneous broadening in the optical spectra; and they will cause formation of local phonon modes that can interact strongly with electronic states.

CHAPTER – 4

Growth and characterization of DMPP (3-(2,3-dimethoxyphenyl)-1-(pyridin-2-yl)prop-2-en-1-one) Single Crystal

1. Introduction

Organic nonlinear optical materials are expected to be active materials for optical communication and optical electronics because of their applications in high-speed and high-density data processing. Second order nonlinear optical materials are used in optical switching, frequency conversion and electro optical applications. Recently much progress has been made in the development of new NLO organic materials having large nonlinear optical coefficients. The desire to utilize the properties of these materials has created need for new materials with very large second order susceptibilies for various applications. Among many organic compounds reported for their second harmonic generation, chalcone derivatives are noticeable materials for their excellent blue light transmittance and good crystallizability. This chapter deals with the growth of new chalcone material 3-(2,3-dimethoxyphenyl)-1-(pyridin-2-yl)prop-2-en-1-one (DMPP) and its characterization using single crystal X-ray diffraction analysis, FTIR, UV absorption, TG/DTA, and Second Harmonic Generation (SHG) measurements.

2.2. Material Synthesis and crystallization

2.2.1 Studies of solubility of DMPP with different solvents

In solution growth technique, the selection of solvent plays a very important role in growing superior quality single crystals of organic compounds. The interaction between the solvent and solute molecules in the

solution and also between the solvent and the crystal surface play a major role in determining the growth rates and also the morphology of the crystal. An anisotropic growth behavior was observed in organic single crystals because of high polar nature and also due to the effects of molecular interaction in solutions. Therefore appropriate selection of solvents is a key factor for the successful growth of single crystals of organic nonlinear optical materials. In this view solubility studies have been carried out for the appropriate selection of solvent for the growth of high quality DMPP crystal. A known amount of acetone 20ml was taken in a conical flask and was immersed in a temperature controlled bath provided with a stirrer. Once the temperature of the solvent reached the bath temperature, a known amount of DMPP powder was added while stirring the solvent. The addition of the DMPP powder was continued until it stops dissolving. The weight of DMPP added into the solvent was calculated by recording the initial and final weights, which gives the solubility of DMPP in acetone for the bath temperature. Similarly the solubility the solubility of the DMPP was determined above the room temperature using this procedure. The same procedure was carried out to determine the solubility of DMPP in methanol and DMF solvents. The solubility of the compound varies almost linearly with temperature for all the three solvents as shown in the figure 2.1. For the growth of superior quality DMPP crystal, moderately soluble solvent acetone was selected.

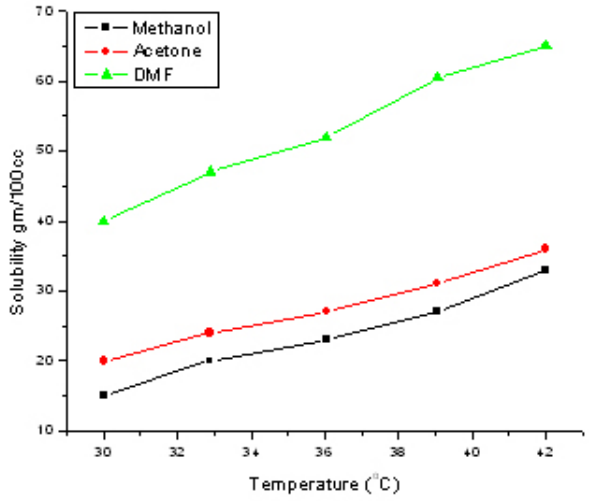

Figure 2.1 Variation of Solubility with temperature for DMPP crystal

2.2.2 Synthesis and crystal growth

DMPP was synthesized by a Claisen–Schimidt condensation reaction [11]. This is the reaction of substituted acetyl pyridine with substituted benzaldehyde in the presence of an alkali. To synthesize DMPP, commercially available Analytical Reagent (AR) grade chemicals were used. 2-Acetyl pyridine (0.01 mol) and 2,3-Dimethoxybenzaldehyde (0.01 mol) was dissolved in methanol (60 ml). Sodium hydroxide (5 ml, 20%) was then added drop wise to the solution, and it stirred for 1.5 hr. The content of the flask were poured into ice-cold water, and the resulting crude solid was collected by filtration. The compound was dried and re-crystallized twice with acetone. The purity of the compound was checked by thin-layer chromatography. To avoid microbes charcoal has been added to the solution.

Crystals were grown by the slow evaporation technique at room temperature using acetone as a solvent. An aqueous solution of DMPP was prepared in a vessel and covered with a perforated sheet, and kept in a dust free atmosphere for solution evaporation. At the period of super saturation, tiny crystals were nucleated in the vessel. Tiny crystals were allowed to

grow to a maximum possible dimension and then harvested. The crystals reached a maximum size of 20 x 2 x 2mm^3 in a period of two weeks. Crystals obtained were slight greenish in colour, non-hygroscopic and stable at room temperature as in the figure 2.2a.

2.2.3 **Morphology studies**

The chalcone crystals are very difficult to grow into sufficient size and quality. Inclusion of solvent into the crystal was a major problem in organic compounds. Therefore in this chapter the crystal growth and optimized condition for the growth of single crystals are described. The morphology was indexed using winXMorph crystal morphology indexing program and as shown in figure 2.2b. The single crystal XRD data was used as input to draw morphology. The winXMorph program indexed planes are confirmed by the single crystal XRD morphology indexing technique.

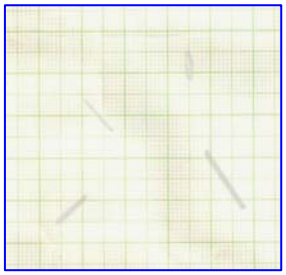

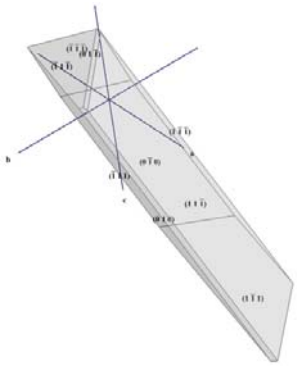

Figure 2.2a Single crystals of DMPP Figure 2.2b Morphology of DMPP

2.3 Crystal structure determination using XRD

A good quality single crystal of DMMP was selected under a polarizing microscope for data collection on an Oxford X calibur, Eos(Nova) CCD diffractometer. The X-ray generator was operated at 50 kV and 1 mA using enhanced Mo Kα radiation. Data were collected with a scan width of 1°. The data reduction, an empirical absorption correction, and space group

determination were carried out using CrysAlisPro RED. The crystal structure was solved by direct methods and refined by full matrix least-squares method using SHELXL97, in the WinGx package suite. The positions of all hydrogen atoms were fixed geometrically and refined isotropically using the riding atom model. Geometrical and intermolecular interactions analysis were done using PARST95 and PLATON.

Compound DMMP (Figure 2.3) is crystallized in orthorhombic non-centrosymmetric space group $Pca2_1$ with Z = 4. The adoption of non-centrosymmetic space group by DMMP is supported by higher SHG activity. The crystal structure is stabilized by weak C–H···O and C–H···N intermolecular interactions in the crystalline lattice (Table 2.1). Weak C–H···O intermolecular interactions involving carbonyl oxygen O_1 and H_2 and methoxy oxygen O_2 and H_{11} form an infinite molecular chain along the crystallographic 'c' axis whereas C–H···N intermolecular interactions further enhance the stability of packing (Figure 2.4). The details of the crystal data and refinement are given in Table 2.2.

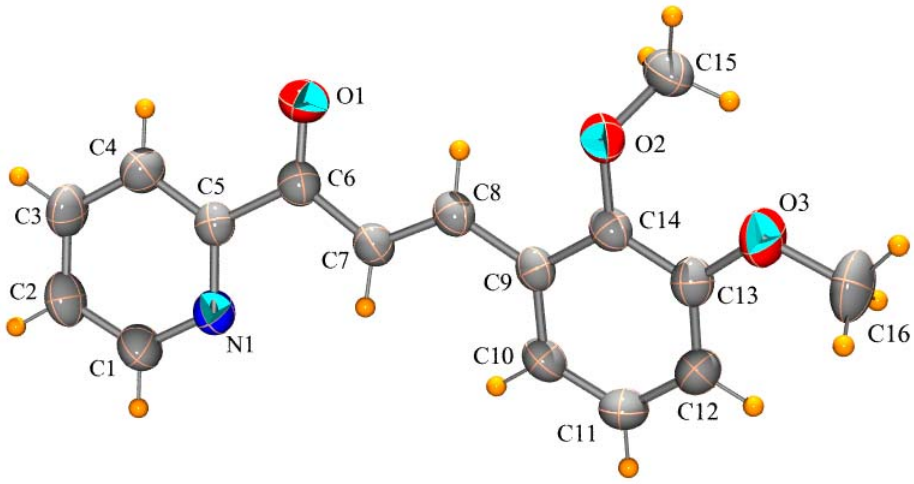

Figure 2.3 ORTEP of DMPP drawn with 50% probability and H atoms are shown as small spheres of arbitrary radii.

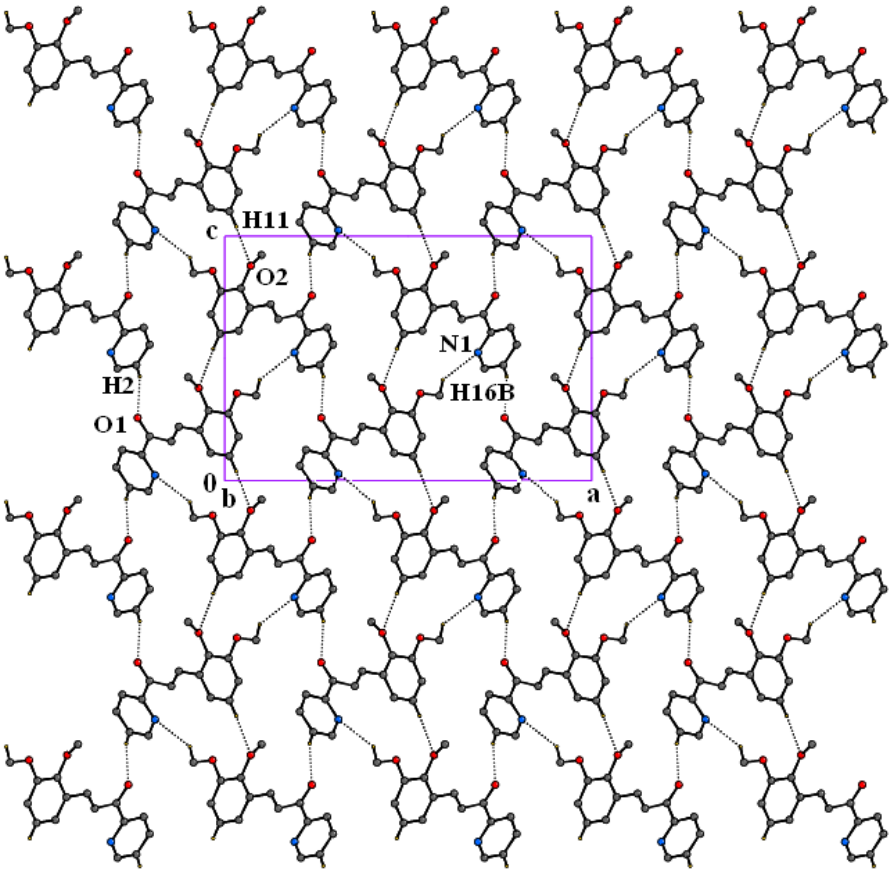

Figure 2.4: A packing diagram of DMPP displaying C–H···O and C–H···N intermolecular interactions in the crystalline lattice. H atoms not involved in the interactions have been omitted for clarity.

Table 2.1: Geometries of Intermolecular Interactions obtained from structural analysis of DMMP.

Interactions	**X–H (Å)**	**H···A (Å)**	**X···A (Å)**	**X–H···A (°)**	**Symmetry**
C2–H2···O1	0.930	2.590	3.471(3)	157.0	−X−1/2, Y+1, Z−1/2
C11–H11···O2	0.930	2.560	3.376(3)	147.0	−X−1, −Y+1, Z−1/2
C16–H16B···N1	0.960	2.580	3.402(4)	143.0	−X−1, −Y+1, Z+1/2

Table 2.2: Crystallographic and experimental details of DMPP.

Molecular formula	$C_{16}H_{15}NO_3$
Formula weight	269.29
Crystal shape and colour	block, slight greenish
Crystal System	Orthorhombic
Space group	$Pca2_1$
a (Å)	20.3106(8)
b (Å)	4.9574(2)
c (Å)	13.4863(5)
Volume, Z	1357.91(9) $Å^3$, 4
λ (Å)	0.71073 (Mo-K_α)
T (K)	295
Reflections measured	8258
Unique reflections	2563
$R_1(F^2)$, $wR_2(F^2)$	0.0397, 0.0852
Goodness-of-fit	1.066
$\nabla\rho_{min, max}$ ($eÅ^{-3}$)	–0.113, 0.177

2.4 Characterization

2.4.1 Elemental analysis (Carbon, Hydrogen and Nitrogen)

To confirm the chemical composition of DMPP, CHN, analysis was carried out on the re-crystallized sample using the Elementar Vario EL III CHNS analyzer. The result of the analysis is presented in Table 2.3. Theoretical values of CHN were found by the molecular formula

$C_{16}H_{15}NO_3$. The experimental and calculated values of C, H, and N agree with each other, confirming the formation of $C_{16}H_{15}NO_3$.

Table 2.3: CHN Analysis of DMPP

Element	Experimental (%)	Computed (%)
Carbon	64.5	64.2
Hydrogen	5.01	5.05
Nitrogen	4.65	4.67

2.4.2 Density and melting point measurement

Crystal purity has been confirmed by density measurement. The density of the compound was measured using Archimedes's principle, and it was found to be 1.17g/cm^3. The melting point, determined by using the capillary tube method, was found to be 80^{o}C.

2.4.3 FT-IR spectral analysis

The FT-IR analysis of DMPP was carried out to investigate the presence of functional groups and their vibrational modes. The sample was prepared by mixing DMPP with KBr pellet. The spectrum was recorded between 400 cm^{-1} and 4000 cm^{-1} using a BRUKER 66V FT-IR spectrometer and the spectrum is shown in Figure 2.5. The FT-IR spectrum confirms the formation of DMPP and its characteristic frequencies and the corresponding assignments are recorded in Table 2.4.

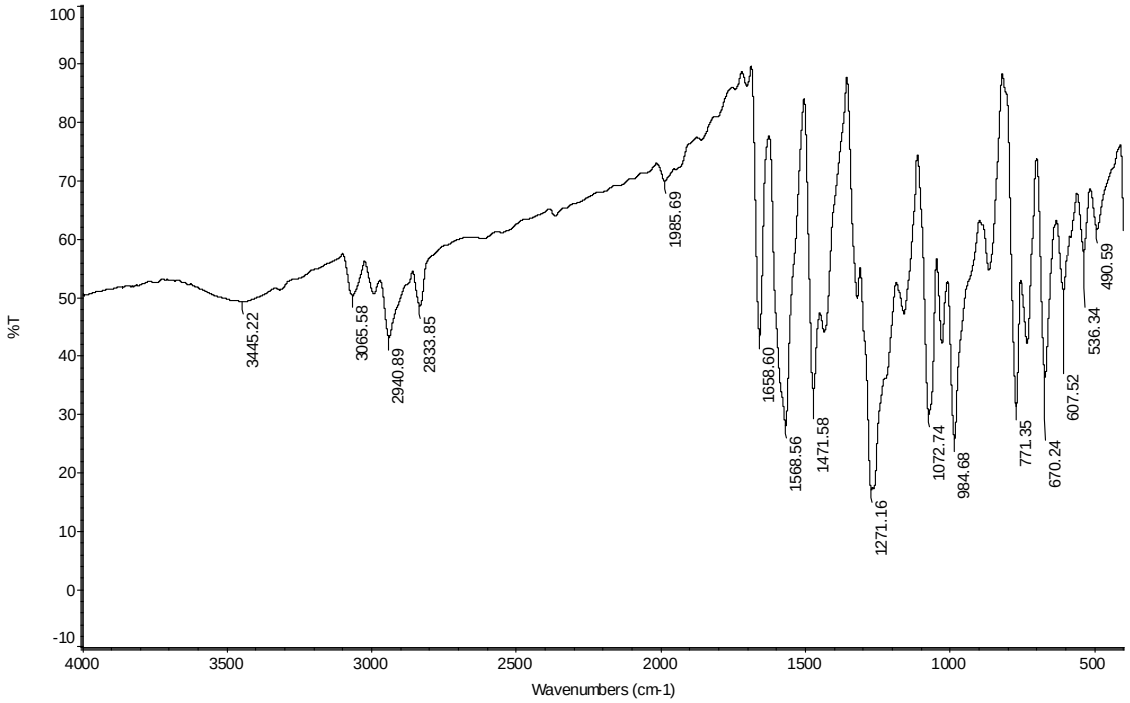

Figure 2.5: FTIR spectrum of DMPP crystal

Table 2.4: Assignment of vibrational frequencies

Wave number(cm^{-1})	Assignment
3066.58, 2940.89	asymmetric & symmetric C-H stretching
& 2833.85	of methyl group
1985.69	combination and week overtone band
1658.60	C=O stretching vibration
1568.56	C=C aromatic stretching
1471.58	C-H bending vibrations
1271.6	aryl C-O stretching (asymmetric C-O-C stretching)
1072.74	symmetric C-O-C stretching vibrations
	(alkyl C-O stretching)
984.68& 771.35	characteristic C-H out-of-plane aromatic bending

2.4.4 Spectroscopic studies

Three wavelength regions of transparency are of interest in the definition of non-linear optical (NLO) materials for frequency conversion; far-UV(<200nm), visible (350-700nm) and NIR (ca. 1200 nm). The far UV NIR regions are well served by inorganic compounds and semiconductors compounds [19]. Most of the organic NLO materials having optical absorption edge in the 400 nm region are used to develop a blue-violet frequency conversion. UV–vis–NIR absorption spectrum of the crystal was recorded using a SECOMOM ANTHELIE 70M UV–VIS spectrophotometer in the wavelength range of 200–1000 nm. A solution of DMPP in DMF was placed in a 1 cm cuvette for measurement. The recorded spectrum is shown in Figure. 2.6. The crystal has a wider transparency range extending into the entire visible and IR region (cut off 400nm). As the entire region does not bear any absorption band, it may be used for NLO applications.

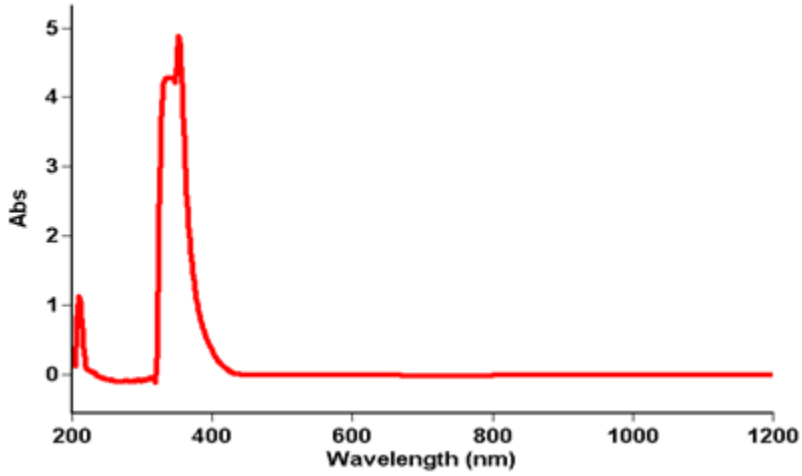

Figure. 2.6 Optical absorption spectrum DMPP crystal

2.4.5 Thermal studies

Thermal studies such as DT and TG have been carried out for DMPP crystal in the range of 28^{o}C to 913^{o}C in nitrogen atmosphere is shown in Figure 2.7. The DTA curve implies that first endothermic peak at 79.49^{o}C

which corresponds to the melting point of the crystal. The broad endothermic peak from 270°C to 400°C corresponds to the first phase of TG curve indicating the major decomposition of the sample.

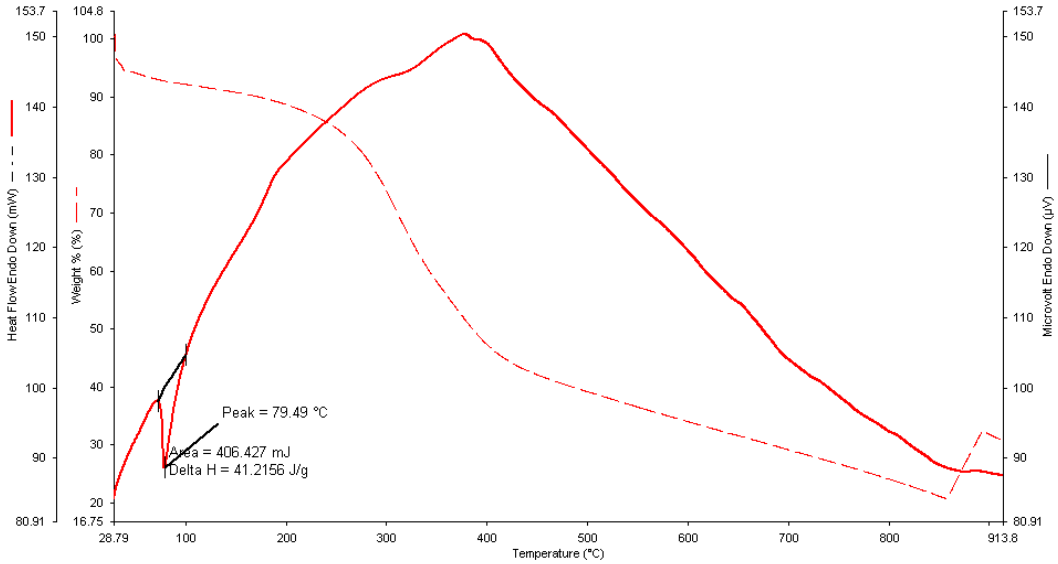

Figure 2.7: TG/DTA curve of DMPP crystal

2.5 Nonlinear optical studies

2.5.1 Second harmonic generation

A Q-switched Nd:YAG laser beam of wavelength 1064 nm, with beam energy of 4mJ/pulse is used. The DMPP crystal was powdered and packed in a micro-capillary of uniform bore and exposed to laser radiations. The output from the sample was monochromated to collect the intensity of 532nm component, and to eliminate the fundamental wavelength. Second harmonic radiation generated by the randomly oriented micro crystals was focused by a lens and detected by a photo multiplier tube. The generation of the second harmonic was confirmed by the emission of green light. A sample of urea and KDP, are also powdered to the same particle size as the experimental samples, was used as a reference material for the present

measurement. The SHG conversion efficiency of DMPP crystal was found to be equal to that of KDP crystal.

2.5.2 Third harmonic generation

[1] The DMPP crystal was dissolved in AR grade DMF and the concentration of the solution was 1.0 x 10^{-3} mol/L. The sample was taken in a quartz cuvette of thickness 1 mm for the Z-Scan measurements. Single beam Z-scan technique was employed to measure the third-order optical nonlinearities of the crystal. The experiments were performed using a frequency-doubled, Q-switched Nd: YAG laser (Spectra-Physics GCR170) which produces 7-ns pulses at 532 nm and at a pulse repetition rate of 10 Hz. The input peak-intensity was 2.39 GW/cm^2. The nonlinear transmission of the DMPP was measured with and without the aperture in front of the detector in the far-field using Laser Probe Rj-7620 energy meter with pyroelectric detectors.

By moving the sample on either side of focal point of the laser beam, the open aperture nonlinear transmission of the sample was measured. From observed data the nonlinear absorption coefficient (β) was determined. The open aperture curve of sample is shown in figure 2.8a.

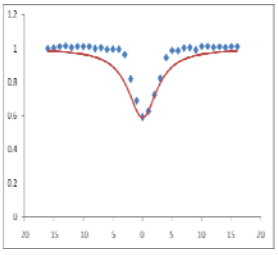

Figure 2.8(a) Open aperture curve

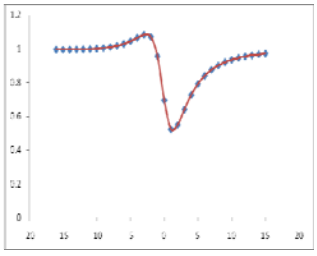

Figure 2.8(b) Closed aperture curve of DMPP crystal

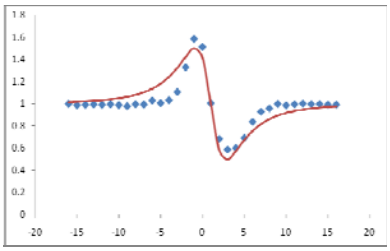

Figure 2.8(c) Pure nonlinear refraction curve

Figure 2.8(a) shows that Intensity dependent absorption indicates that open aperture transmittance curve is symmetric with respect to focus and has minimum transmittance at the focus. The open and closed aperture Z-scan curves obtained for laser pulse for DMPP solution is as shown in figure 2.8(a) and figure 2.8(b). The sample solution has little absorption. The absorption at nanosecond laser pulses contributes cascaded nonlinearity. Moreover the nonlinear absorption in organic molecule is due to two photon induced excited state absorption and hence a measured effective value represents the magnitude of the nonlinear coefficient of the sample.

The normalized transmittance T(z) for the open aperture Z-scan is given by

$$T(z) = \frac{\ln[1+q_0(z)]}{q_0(z)} \quad \text{for } |q_0(z)| < 1 \qquad (1)$$

where,

$$q_0(z) = \frac{I_0\beta(1-e^{-\alpha L})}{(1+z^2/z^2{}_0)\alpha} \qquad (2)$$

and L is the thickness of the sample, α is the linear absorption coefficient, z_0 is the Rayleigh length and I_0 is the on-axis peak irradiance at the focus.

Now the nonlinear absorption coefficient β, is related to the imaginary part of third-order nonlinear optical susceptibility through the equation (1),

$$\text{Im}\,\chi^{(3)} = n_0^2 \varepsilon_0 c\lambda\beta / 2\pi, \qquad (3)$$

where n_0 is the linear refractive index, c is speed of light in vacuum and ε_0 is the permittivity of free space.

From the open aperture Z-scan data, the measured values of nonlinear absorption coefficient (β) and the imaginary part of third-order nonlinear optical susceptibility $\chi^{(3)}$ of the sample are 4.800 cm/GW and 7.39x 10^{-14} esu, respectively.

To obtain a pure nonlinear refraction curve, the division method is adopted as described in. The sample was found to exhibit peak-valley characteristic, indicating negative nonlinear refraction or self-defocusing effect shown in figure 2.8(c). The nonlinear refractive index γ (in m^2/W) is given by the equation (1),

$$\gamma = \frac{\Delta\phi_0 \lambda}{2\pi L_{\text{eff}} I_0}(m^2 / W), \qquad (4)$$

where, $L_{\text{eff}} = \frac{(1-\exp^{-\alpha L})}{\alpha}$ and $\Delta\Phi_0$ is the on-axis phase change given by the equation,

$$\Delta\phi_0 = \frac{\Delta T \text{p-v}}{0.406(1-S)^{0.25}} \quad \text{for } |\Delta\phi_0| \le \pi, \quad (5)$$

Here ΔT_{p-v} is the peak to valley transmittance difference and S is the linear aperture transmittance. Then nonlinear refractive index n_2 (in esu) is related to γ (m^2/W) by,

$$n_2 \text{ (esu)} = (cn_0 / 40\pi)\gamma \text{ (m}^2 / \text{W)}, \qquad (6)$$

The normalized transmittance for pure nonlinear refraction is given by,

$$T(Z) = 1 - \frac{4x\Delta\phi_0}{[(x^2+9)(x^2+1)]}, \qquad (7)$$

where $x = (z/z_o)$. The nonlinear refractive index n_2 (in esu) is related to the real part of third-order nonlinear optical susceptibility through the equation (1),

$$\mathrm{Re}\,\chi^{(3)} = 2n_0^2\varepsilon_0 c n_2, \text{ (esu)} \qquad (8)$$

From the pure nonlinear refraction Z-scan data, the nonlinear refractive index n_2 and real part of third-order nonlinear optical susceptibility $\chi^{(3)}$, for the sample have been calculated to be -2.963x 10^{-11} esu and -31.74x 10^{-14} esu, respectively. The high β_{eff} value of the DMPP sample shows that, it is a promising material for NLO application.

CHAPTER – 5

Growth and characterization of DCPP (3-(2,3-dichlorophenyl)-1-(pyridin-2-yl)prop-2-en-1) single crystal

1. Introduction

Non-linear optical (NLO) organic materials found many applications because of their high conversion efficiency compared to that of inorganic NLO materials. Chalcones are interesting organic NLO materials shows, good crystallizability, high second harmonic generation (SHG) conversion efficiency compared to urea and transparency extending down to the blue region. It has been generally understood that the second-order molecular nonlinearity can be enhanced by large delocalized π-electron systems with strong donor and acceptor groups. The basic strategy of using electron-donor and electron-acceptor substituents to polarize the π-electron system of organic materials has been illustrious for developing the NLO chromophores possessing large molecular nonlinearity, good thermal stability, improved solubility and processability. The SHG can also be improved by the substitution of a donor group on the para position of the benzoyl group instead of an electron acceptor group Wu et al. suggested from their theoretical hyper-polarizability studies on these molecules that the carbonyl group present at the middle in these molecules splits the conjugated system into relatively two independent parts. Therefore, chalcones can be regarded as cross-conjugated molecules that possess two independent hyperpolarizable parts to have a two-dimensional β character. It was also suggested by Zhao et al., and Wuetal., that electron donors such as -OCH_3, -CH_3, -Cl and -Br are the best donor groups for enhancing SHG in

chalcones. Several chalcone molecules have been synthesized and reported for their SHG property.

In this paper we present our experimental results on the crystal growth, characterization and structure-NLO property relationship in chlorine substituted chalcone 3-(2,3-dichlorophenyl)-1-(pyridin-2-yl)prop-2-en-1-one (DCPP) single crystals.

2. Experimental procedure

2.1. Synthesis of the compound

DCPP was synthesized by a Claisen–Schimidt condensation reaction. This is the reaction of substituted acetyl pyridine with substituted benzaldehyde in the presence of an alkali. To synthesize DCPP commercially available Analytical Reagent (AR)-grade chemicals, 2-Acetyl pyridine (0.01 mol) and 2,3 dichlorobenzaldehyde (0.01 mol) were dissolved in methanol (60 ml). Sodium hydroxide (5 ml, 20%) was then added drop wise to the solution, and stirred for 2 h. The contents of the flask were poured into ice-cold water, and the resulting crude solid was collected by filtration. The compound was dried and re-crystallized twice with dimethylformamide (DMF). The purity of the compound was checked by thin-layer chromatography. To avoid microbes charcoal has been added to the solution.

2.2. Crystal growth

The solubility of the compound is determined by adding the solvent to a known amount of compound till it is completely dissolved. It is found that the synthesized compound is insoluble in water, sparingly soluble in benzene and acetone. It is also moderately soluble in DMF. Crystals were grown by the slow evaporation technique at room temperature by using DMF as a solvent. Solution of DCPP was prepared in a vessel covered with perforated

sheet, and kept in a dust free atmosphere. At the period of super saturation, tiny crystals were nucleated. They were allowed to grow to a maximum possible dimension and then harvested. Thus grown needle shaped transparent crystals of dimension 10 x 0.5 x 0.5mm are shown in Fig. 1.

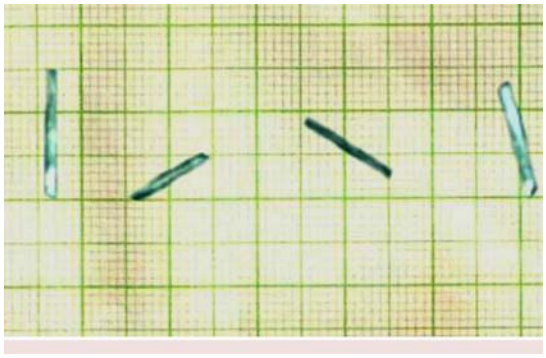

Fig. 1.DCPP single crystal

3. **Characterization**

3.1. CHN analysis

To confirm the chemical composition of DCPP, CHN, analysis was carried out on the re-crystallized sample using the Elementar Vario EL III CHNS analyzer. The result of the analysis is presented in Table 1. Theoretical values of CHN were found by the molecular formula $C_{14}H_9Cl_2NO$. The experimental and calculated values of C, H, and N agree with each other, confirming the formation of $C_{14}H_9Cl_2NO$.

Table 1
CHN Analysis of DCPP

Element	Experimental (%)	Computed (%)
Carbon	60.43	60.46
Hydrogen	3.23	3.26
Nitrogen	5.00	5.04

3.2. Crystal structure determination

Single crystal of DCPP was selected under a polarizing microscope and subjected to single crystal diffraction data collection using an Oxford Xcalibur, Eos(Nova) CCD diffractometer. The X-ray generator was operated at 50 kV and 1 mA using enhanced Mo Kα radiation. The complete data sets were measured with a scan width of 1°. The data reduction, an empirical absorption correction, and space group determination were carried out using CrysAlisPro RED. The crystal structure was solved by direct methods and refined by full matrix least-squares method using SHELXL97, in the WinGx package suite (Version 1.80.05. The positions of all hydrogen atoms were fixed geometrically and refined isotropically using the riding atom model. Geometrical and intermolecular interactions analysis were done using PARST95 and PLATON. The crystallographic details are provided in Table 2.

Table 2

Crystal structure details of DCPP.

Molecular formula	$C_{14}H_9Cl_2NO$
Formula weight	278.12
Crystal shape and colour	block, Pale Blue
Crystal System	Monoclinic
Space group	$P2_1$
a (Å)	7.4229(2)
b (Å)	3.9889(1)
c (Å)	21.2685(6)
β (°)	98.212(2)

Volume ($Å^3$), Z	623.29(3), 2
λ (Å)	0.71073 (Mo-K_α)
T (K)	296(2)
Reflections measured	11330
Unique reflections	2613
$R_1(F^2)$, $wR_2(F^2)$ [$I>2\sigma(I)$]	0.0420, 0.0966
Goodness-of-fit	1.036
Flack parameter	0.10(8)
$\nabla\rho_{min, max}$ ($eÅ^{-3}$)	–0.195, 0.187

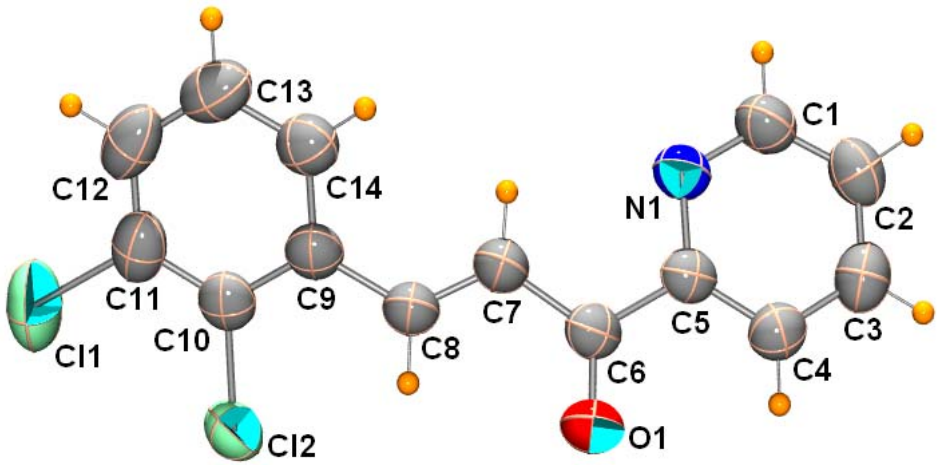

Fig. 2. ORTEP of the molecule with 50% ellipsoidal probability and H atoms are shown as small spheres of arbitrary radii.

The compound (Fig. 2) is crystallized in space group $P2_1$ with Z = 2. The high SHG conversion efficiency observed in this compound might be attributed to the arrangement of molecules in the $P2_1$ space group. It is interesting to note that the dihedral angle between pyridinyl ring and

dichlorophenyl ring is 33.13(1)°, which indicates the non-planar geometry of the crystal structure. The analysis of weak intermolecular interactions reveals that the crystal structure in the crystalline lattice is held together by weak intermolecular C–H···O hydrogen bond (involving carbonyl oxygen O1 and hydrogen atom H3) along a 2_1 screw axis in crystallographic 'b' axis (Fig. 3 and Table 3). In addition, the crystal structure is further stabilized by very weak aromatic stacking interactions (Fig. 3).

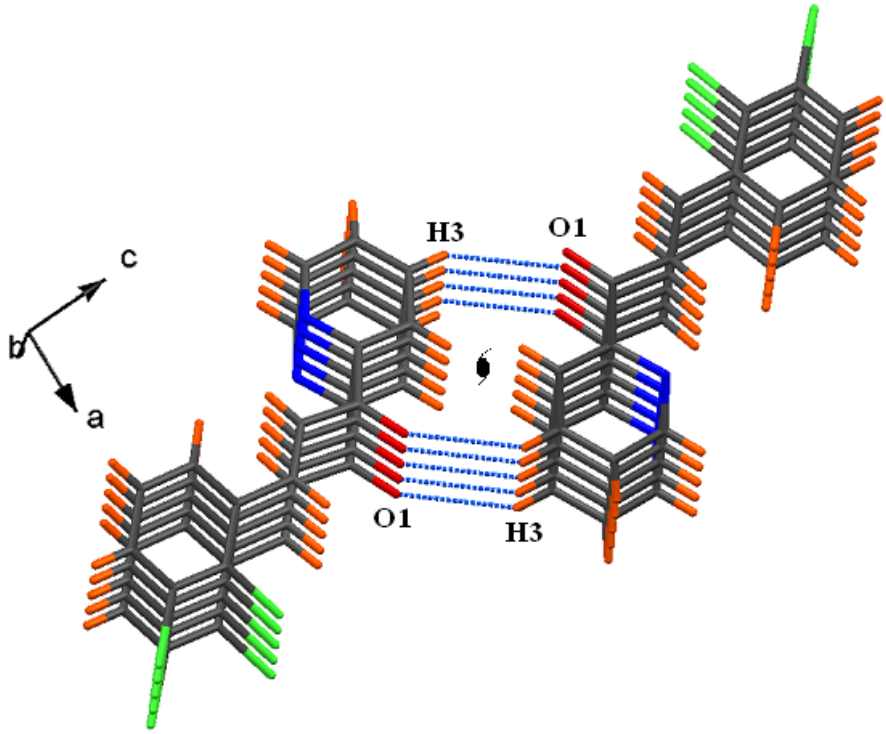

Fig. 3. A packing diagram of molecule depicting C–H···O intermolecular hydrogen bond along 2_1 screw axis in crystallographic 'b' axis.

Table 3

Geometries of Intermolecular Interactions obtained from structural analysis.

Interactions	**X–H (Å)**	**H···A (Å)**	**X···A (Å)**	**X–H···A (°)**	**Symmetry**
C3–H3···O1	0.930	2.687	3.444(4)	139.0	–X+2, Y+1/2, –Z+1

3.3. Density and melting point measurement

The density of the compound was measured using Archimedes's principle, and it was found to be 1.35gmcm^{-3}. The melting point, determined by using the capillary tube method, was found to be 143^{o}C.

3.4. Thermal studies

Thermal studies such as DT and TGA have been carried out for DCPP crystal in the range of 34^{o}C to 811^{o}C in nitrogen atmosphere and the results are shown in Fig. 4.

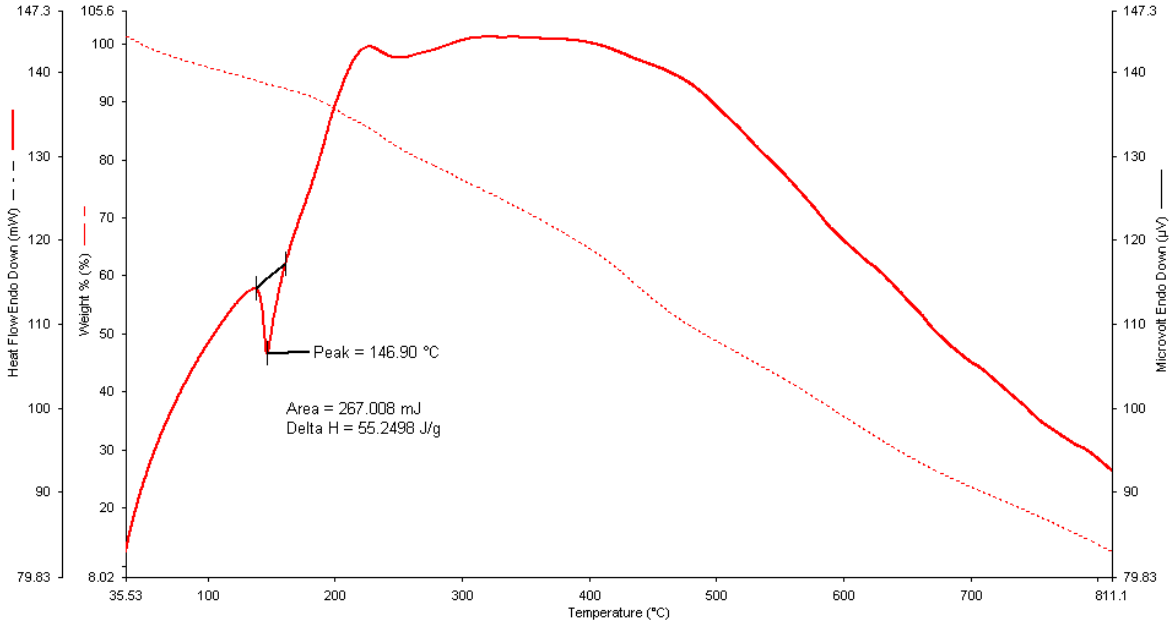

Fig. 4. TGA/DTA curve of DCPP crystal

It shows that the sample is stable till 140^{o}C. Beyond that it undergoes an endothermic transition, which corresponds to the melting point of the material. Thermo-gravimetric analysis shows the softening of the DCPP at 142^{o}C accompanied by a loss of material.

3.5. Powder SHG measurement

A Q-switched Nd:YAG laser with a pulse energy of 4.95mJ/pulse was used as a source. Microcrystalline powdered sample of DCPP was tightly packed in a glass capillary and exposed to a fundamental wave with a pulse width of 10 ns, repetition frequency10 Hz, and a wavelength of 1064 nm. The generated second harmonic wave of 532 nm was detected by a photomultiplier tube and converted into electrical signal. The electrical signal was displayed on the oscilloscope. The signal amplitudes in volts indicate the SHG efficiency of the sample. The SHG conversion efficiency of DCPP crystal was found to be 4 times that of KDP.

3.6 Optical studies

3.6.1 FT-IR spectral analysis

The FT-IR analysis of DCPP was carried out to investigate the presence of functional groups and their vibrational modes. The sample was prepared by mixing DCPP with KBr pellet. The spectrum was recorded between 400 cm^{-1} and 4000 cm^{-1} using a BRUKER 66V FT-IR spectrometer and the spectrum is shown in Fig. 5.

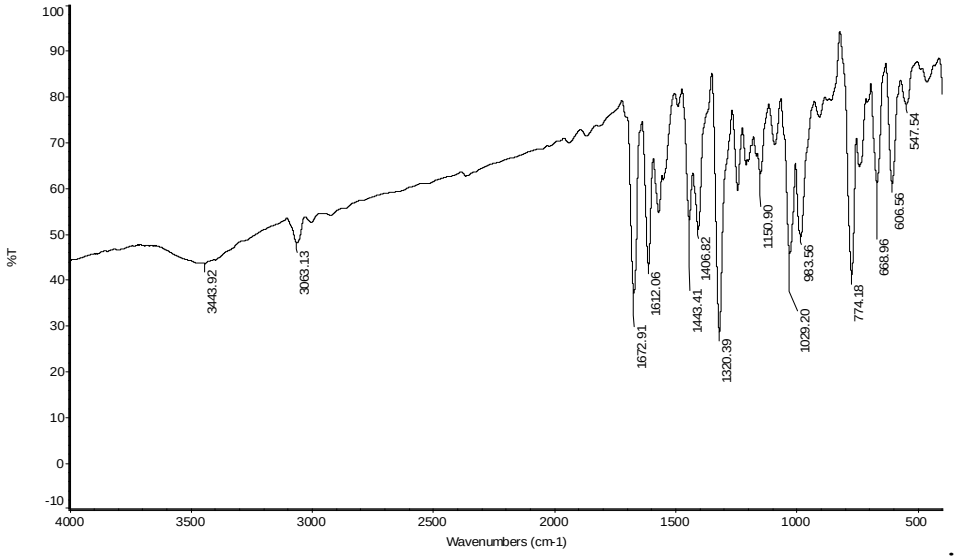

Fig. 5. FTIR spectrum of DCPP

The FT-IR spectrum confirms the formation of DCPP and its characteristic frequencies and the corresponding assignments are recorded in Table. 4.

Table 4

Assignment of vibrational frequencies

Wave number(cm^{-1})	Assignment
3443.92	N-H stretching
3063.13	C-H Stretching of methyl group
1672.91	C=O stretching vibration
1612.02	aromatic C=C vibration
1443.41, 1406.82 & 1320.39	alkyl C-H bending vibrations
1150.9	C-H wagging
1029.2	C-Cl stretching vibrations
983.56, 774.18	Characteristic C-H out-of-plane aromatic bending
668.96, 606.56	C-H bending

3.6.2. UV–vis–NIR spectrum

Optical transparency is one of important parameter that a NLO material posses. Wider transparency is needed for most of the practical applications. UV–vis–NIR absorption spectrum of the crystal was recorded

using a SECOMOM ANTHELIE 70M UV–VIS spectrophotometer in the wavelength range of 200–1000 nm. A solution of DCPP in DMF was placed in a 1 cm cuvette for measurement. The recorded spectrum is shown in Fig. 6.

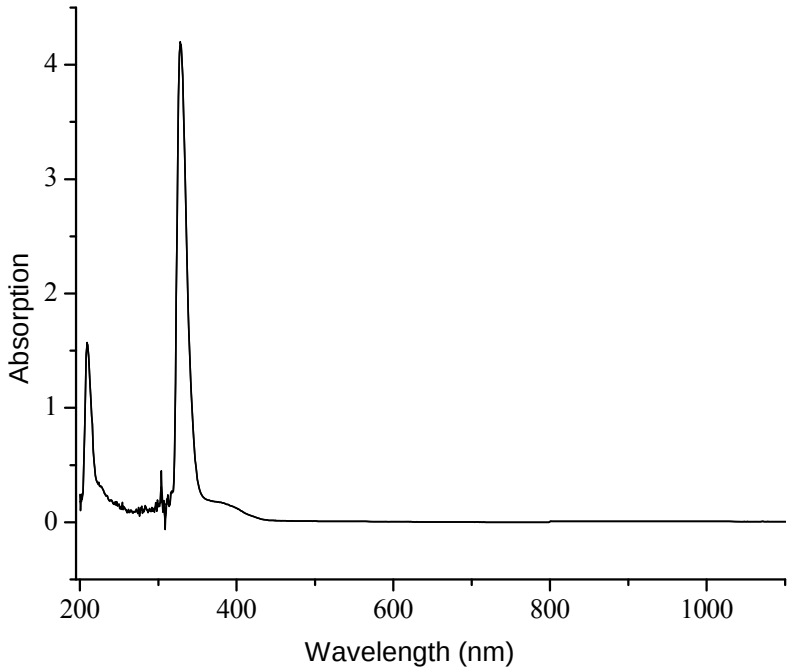

Fig. 6. Optical absorption spectrum of DCPP crystal

The crystal has a wider transparency range extending into the entire visible and IR region (cut off 350nm). As the entire region does not bear any absorption band, it can be used for NLO applications.

CHAPTER – 6

CONCLUSIONS

In this project growth and characterization of two new chalcone derivates have been carried out and the results of the analysis were discussed.

The new NLO optical chalcone derivative, DMPP was synthesized and single crystals of this compound was successfully grown by the solution growth technique at room temperature using acetone as a solvent. FT-IR is used to confirm the functional groups of the grown crystal. Single-crystal XRD studies were carried out to determine the cell parameters. The UV–VIS–NIR spectrum reveals that, in the crystal, the absorption takes place in the UV region and the crystal is transparent in the entire visible region. This crystal has powder SHG conversion efficiency equal to that of KDP. DMPP crystal is thermally stable up to 79.49^0C, and can be suggested for NLO applications below 80^0C. Due to the presence of a wide transparency range and the values obtained from Z-scan measurements, confirms the potential use of this sample for NLO application.

The new NLO optical chalcone derivative, DCPP was synthesized and single crystals of this compound were successfully grown by the solution growth technique at room temperature using DMF as a solvent. FT-IR is

used to confirm the functional groups of the grown crystal. Single-crystal XRD studies were carried out to determine the cell parameters. The UV–VIS–NIR spectrum reveals that, in the crystal, the absorption takes place in the UV region and the crystal is transparent in the entire visible region. This crystal has a powder SHG conversion efficiency of 4 times that of KDP. Due to the presence of a wide transparency range and higher second harmonic efficiency the crystal may be used for NLO applications. DCPP crystal was stable up to 140^0C, and can be suggested for NLO applications below 140^0C.

CHAPTER – 7

REFERENCES

[1] Ch. Bosshard, R. Spreiter, L. Degiorgi, P. Gunter, Phys. Rev. B66 (2002) 205107.

[2] B. Zhao, W.-Q. Lu, Z.-H. Zhou, Y. Wu, J. Mater. Chem. 10 (2000) 1513.

[3] Y. Goto, A. Hayashi, Y. Kimura, M. Nakayama, J. Crystal Growth 108 (1991) 688.

[4] D. Fichou, T. Watanabe, T. Takeda, S. Miyata, Y. Goto, M. Nakayama, Jpn. J. Appl. Phys. 27 (1988) L249.

[5] Y. Kitaoka, T. Sasaki, S. Nakai, Y. Goto, Appl. Phys. Lett. 59 (1991) 19.

[6] H.J. Ravindra, A.J. Kiran, R.N. Satheesh, S.M. Dharmaprakash, K. Chandrase- kharan, K. Balakrishna, F. Rotermund, J. Crystal Growth 310 (2008) 2543.

[7] H.J. Ravindra, A.J. Kiran, S.M. Dharmaprakash, R.N. Satheesh, K. Chandrase- kharan, K. Balakrishna, F. Rotermund, J. Crystal Growth 310 (2008) 4169.

[8] A.J. Kiran, H.C. Kim, K. Kim, F. Rotermund, H.J. Ravindra, S.M. Dharmaprakash, H. Lim, Appl. Phys. Lett. 92 (2008) 113307.

[9] J. Zyss, Chem. Phys., 1979, 71, 909.

[10] B. F. Levine, C. G. Bethea, C. D. Thurmond, R. T. Lynch and J. L. Berstein, J. Appl. Phys., 1979, 50, 2523.

[11] D.S. Chemla, J. Zyss, Nonlinear Optical Properties of Organic Molecules and Crystals, Academic Press, New York, 1987.

[12] P.N. Prasad, D.J. Williams, Introduction to Nonlinear Optical Effects in Organic Molecules and Polymers, John-Wiley & Sons Inc., New York, 1991.

[13] D. Fichou, T. Watanabe, T. Takeda, S. Miyata, Y. Goto, M. Nakayama, Jpn. J. Appl. Phys. 27 (1988) L249.

[14] D. Wu, B. Zhao, Z. Zhou, J. Mol. Struct. 83 (2004) 682.

[15] B. Zhao, Y. Wu, Z.-H. Zhou, W.-Q. Lu, C.-Y. Chen, Appl. Phys. B 70 (2000) 601

[16] D. Wu, B. Zhao, Z. Zhou, J. Mol. Struct. 83 (2004) 682.

[17] B. Zhao, W.-Q. Lu, Z.-H. Zhou, Y. Wu, J. Mater. Chem. 10 (2000) 1513

[18] D. Fichou, T. Watanabe, T. Takeda, S. Miyata, Y. Goto, M. Nakayama, Jpn. J. Appl. Phys. 27 (1988) L249

[19] T. Uchida, K. Kozawa, T. Sakai, M. Aoki, H. Yoguchi, A. Abduryim, Y. Watanabe, Mol. Cryst. Liq. Cryst. 315 (1998) 135.

[20] A.I. Vogel, in: A.I. Vogel, B.S. Furniss, A.J. Hannaford, P.W.G. Smith, A.R. Tatchell (Eds.), Vogel's Textbook of Practical Organic Chemistry, fifth ed., Longman Group, London, 1999.

[21] J.C. Brice, Crystal Growth from Solution, North-Holland, Amsterdam, 1973.

[22] Oxford Diffraction, CrysAlisPro CCD and CrysAlisPro RED, Versions 1.171.33.34d. Oxford Diffraction Ltd., Abingdon, Oxfordshire, England, 2009

[23] S. M. Sheldrick, Acta Cryst., A64 (2008)112.

[24] L. J. Farrugia, J. Appl. Cryst., 32 (1999) 837.

[25] A. Nardelli, J. Appl. Cryst., 28 (1995) 569.

[26] A. L. Spek, J. Appl.Cryst., 36 (2003) 7.

[27] Leonid V. Azarofft Introduction to solidst (1977).

[28] Brice J. C. "Growth of Crystals from liquids" North Hollandt New York (1973).

[29] Pamphin B.Rt "Crystal Growth" Pergamon Press Oxford (1975) .

[30] Patel A.R, A short course ln solid state physics vol. 1 (1977) 117.

[31] Fan S, Shen G. Wang Wand Lex; J. Crystal growth 99 (1990) 811.

[32] Carrxthere J.R and Wine gard W.C; Crystal growth (Peiser H.S. ed) Pergamon New York (1966) 645.

[33] Schmid F and Viechnicki D; J. Crystal groth 11 (1971) 345.

[34] Tachibana Mt Tang Q, and Kojma Ki Jpn. J. Appl. Physt 31 (1992) 202.

[35] Tachibana M, Wang J.S. and Kojma K; J. Phys. D. Appl. Phys. 26 (1993) B145 .

[36] Rynji Morita and Vidakovic P.V; Appl. Phys. Lett. 61, 24 (1992) 2854.

[37] Baremert J.C, Twieg R.J and Dirk C.W; Appl. Phys. Lett. Sl (1987) 1484.

[38] Fakuda. T. Sano T, Hosaya Sand Yo on D.H; Cryst. Res. Technol. 2~ 7, (1994) 971.

[39] Vere A. W . "Crystal growth Principals and progress" Plenem Press, New York (1987).